Electronic Supplementary Material (ESI) for Polymer Chemistry.

Comprehensive theoretical and experimental study of near infrared absorbing copolymers based on dithienosilole: Supporting Information

Katarzyna Brymora,[a] Wissem Khelifi,[b] Sylvie Blanc,[b] Lionel Hirsch,[c] Antoine Bousquet,[b,*] Christine Lartigau-Dagron,[b,*] and Frédéric Castet[a,*]

[a] *Institut des Sciences Moléculaires (ISM, UMR CNRS 5255), Université de Bordeaux, 351 cours de la Libération, 33405 Talence, France.*

frederic.castet@u-bordeaux.fr

[b] *Universite de Pau et des Pays de l'Adour, E2S UPPA, CNRS, IPREM, Pau, France*

antoine.bousquet@univ-pau.fr; christine.lartigau-dagron@univ-pau.fr

[c] *Laboratoire de l'Intégration du Matériau au Système (IMS, UMR CNRS 5218), Université de Bordeaux, ENSCBP, 16 Avenue Pey-Berland, 33607 Pessac Cedex, France*

1. Computational Results

1.1 Geometrical and electronic properties of monomers

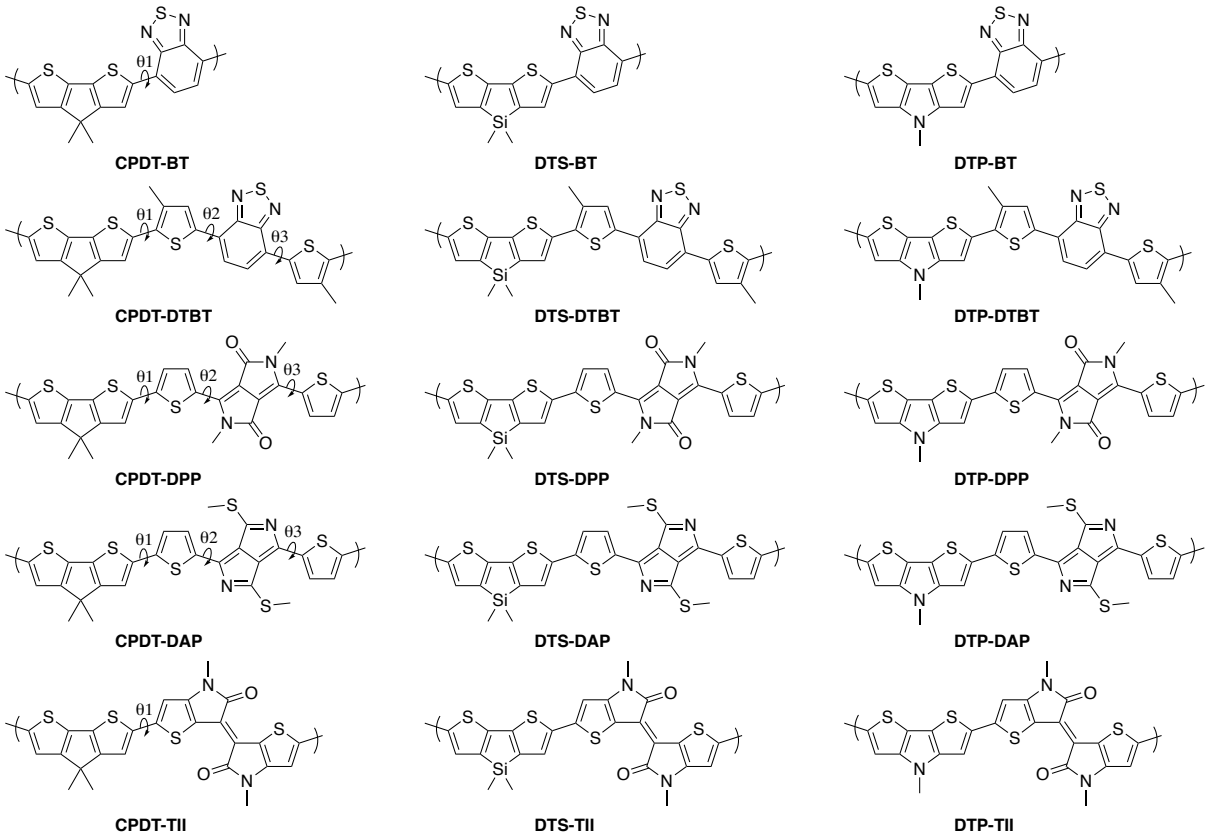

Figure S1.1: Chemical structure of the investigated donor-acceptor (D-A) polymers with definition of torsion angles (θ_1 = S-C-C-C, θ_1 = C-C-C-C and θ_3 = C-C-C-C) and (in red) the conjugated path used to calculate the bond length alternation.

The parameters characterizing the ground-state geometries of the monomers, namely the torsion angles θ around single bonds and the bond length alternation (BLA) along the conjugated backbones (red segments in Figure S1.1), are reported in Table S1.1. For a conjugated chain containing *N* carbon atoms, the BLA is defined as:

$$\mathrm{BLA} = \frac{1}{\mathrm{N}-2}\sum_{\mathrm{i}=1}^{\mathrm{N}-2}\left\{\left(\mathrm{d}_{\mathrm{i}+1,\mathrm{i}+2} - \mathrm{d}_{\mathrm{i},\mathrm{i}+1}\right) \times (-1)^{\mathrm{i}+1}\right\}$$

where $d_{i,j}$ is the interatomic distance between carbons i and j.

Table S1.1: Bond length alternation (BLA, Å) and torsion angles (θ, degrees), as calculated at the M06-2X/6-311G(d) level for the D-A monomers. [a] See Figure S1.1 for the definition of torsion angles.

Monomer	BLA	θ_1	θ_2	θ_3
CPDT-BT	0.059	-24.6	/	/
CPDT-DTBT	0.062	34.6	-16.9	-22.4
CPDT-DPP	0.052	-22.7	0.6	-0.6
CPDT-DAP	0.043	-20.4	2.4	2.3
CPDT-TII	0.050	-24.0	/	/
DTS-BT	0.063	-26.8	/	/
DTS-DTBT	0.064	34.6	-17.1	-22.2
DTS-DPP	0.055	17.9	-1.7	0.7
DTS-DAP	0.045	-16.9	3.8	2.5
DTS-TII	0.054	-25.4	/	/
DTP-BT	0.049	27.4	/	/
DTP-DTBT	0.056	36.5	-16.8	-22.4
DTP-DPP	0.046	23.5	-0.4	0.3
DTP-DAP	0.037	-20.3	3.0	2.4
DTP-TII	0.044	-27.3	/	/

Table S1.2: HOMO and LUMO of DA monomers (with energies in eV), and HOMO-LUMO gaps (E_g, eV) calculated at the M06-2X/6-311G(d) level.

Monomer	HOMO	LUMO	E_{HOMO}	E_{LUMO}	E_g
CPDT-BT	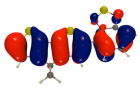	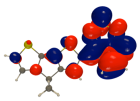	-6.59	-1.76	4.83
CPDT-DTBT	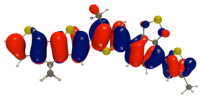	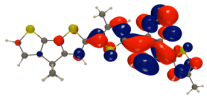	-6.24	-1.96	4.28
CPDT-DPP		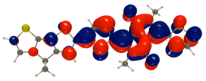	-6.08	-2.08	4.00
CPDT-DAP	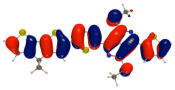	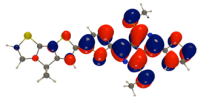	-6.16	-2.62	3.54
CPDT-TII	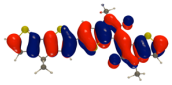	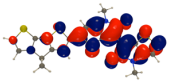	-6.03	-2.03	4.00

Monomer	HOMO	LUMO	E_{HOMO}	E_{LUMO}	E_g
DTS-BT	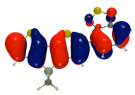	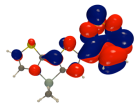	-6.59	-1.76	4.83
DTS-DTBT	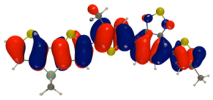	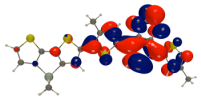	-6.30	-1.95	4.35
DTS-DPP	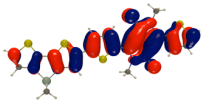	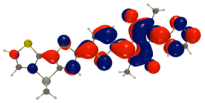	-6.10	-2.08	4.01
DTS-DAP	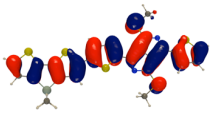	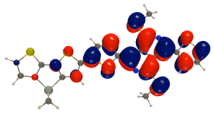	-6.20	-2.62	3.58
DTS-TII	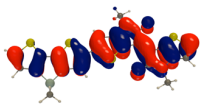	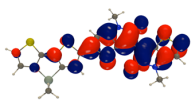	-6.08	-2.03	4.05

Monomer	HOMO	LUMO	E_{HOMO}	E_{LUMO}	E_g
DTP-BT	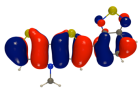	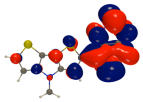	-6.39	-1.71	4.69
DTP-DTBT		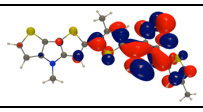	-6.19	-1.94	4.25
DTP-DPP	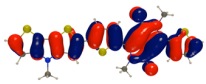	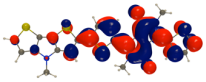	-6.05	-2.05	4.00
DTP-DAP	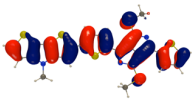	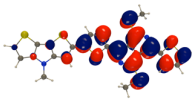	-6.12	-2.61	3.51
DTP-TII	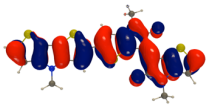	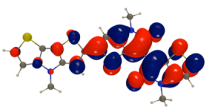	-6.01	-2.01	4.00

Figure S1.2: Electron density difference maps of DA monomers, calculated at the M06-2X/6-311G(d) level. Blue (white) lobes are associated with positive (negative) Δρ values.

	D = CPDT	D = DTS	D = DTP
A = BT	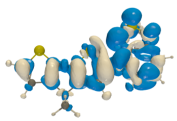	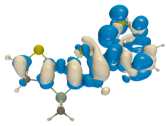	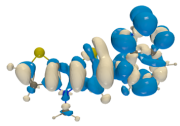
A = DTBT	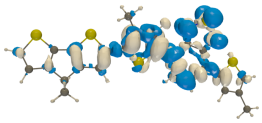	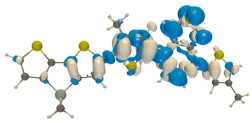	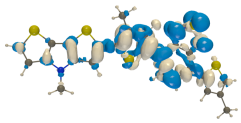
A = DPP	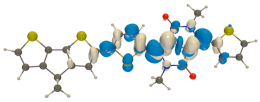	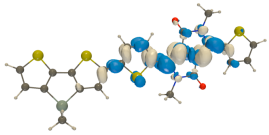	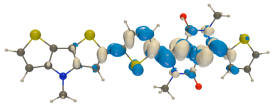
A = DAP	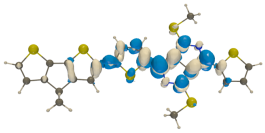	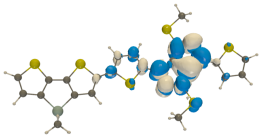	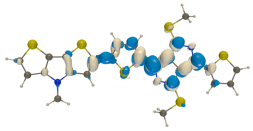
A = TII	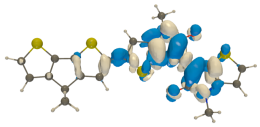	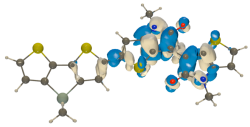	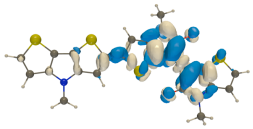

1.2 Electronic and optical properties of increasingly large oligomers, and extrapolation to polymer properties

$S_0 \rightarrow S_1$ transition energies in the polymer limit (ΔE_{01}^{∞}) were evaluated using the 2-parameter fitting equation issued from the Kuhn's coupled oscillator model:

$$E(N) = E_1 \sqrt{1 + D_k \, cos\left(\frac{\pi}{N+1}\right)}$$

where *N* is the number of double bonds along the shortest conjugation pathway connecting the terminal atoms of the oligomer backbone. The fitting parameters, E_1 and D_k , respectively describe the transition energy of a formal double bond, and the relative force constant measuring how strongly the double bonds are coupled through single bonds. As such, E_1 is intrinsically related to the optical gap of the repeating units, while D_k depends on the planarity of the molecular backbone and on the BLA along the π-conjugated skeleton. The limit case $D_k = -1$ corresponds to a situation in which all bonds are identical (BLA = 0) and gives rise to an optical gap equal to zero in the polymer limit.

The $S_0 \rightarrow S_1$ vertical transition energies of increasingly large oligomers are reported in Tables S1.3-S1.7, while their evolution as a function of 1/N is shown in Figure S1.3. The transition energies in the polymer limit (ΔE_{01}^{∞}) are reported in Table S1.8, together with the optimized values of the Kuhn fit parameters E_1 and D_k .

Table S1.3: Transition energies (ΔE_{01}, eV), wavelengths (λ_{01}, nm), oscillator strengths (f_{01}, dimensionless) relative to the $S_0 \rightarrow S_1$ transition, as well as frontier orbital energies and electronic gaps ($E_g = E_{LUMO} - E_{HOMO}$, all values in eV) calculated at the M06-2X/6-311G(d) level for increasingly large $(D\text{-}A)_n$ oligomers with A = BT.

n	ΔE_{01}	λ_{01}	f_{01}	E_{HOMO}	E_{LUMO}	E_g
			CPDT-BT			
1	3.07	404	0.47	-6.47	-1.77	4.71
2	2.46	505	1.45	-6.08	-2.09	3.98
3	2.26	548	2.60	-5.94	-2.22	3.72
4	2.15	576	3.78	-5.87	-2.30	3.58
5	2.10	590	4.88	-5.84	-2.33	3.51
			DTS-BT			
1	3.15	393	0.47	-6.59	-1.76	4.83
2	2.53	490	1.36	-6.18	-2.08	4.10
3	2.35	528	2.41	-6.05	-2.20	3.85
4	2.28	545	3.47	-6.00	-2.25	3.75
5	2.20	563	4.47	-5.95	-2.30	3.65
			DTP-BT			
1	3.08	402	0.45	-6.39	-1.71	4.69
2	2.44	509	1.45	-5.98	-2.05	3.93
3	2.25	550	2.68	-5.85	-2.17	3.68
4	2.15	576	3.87	-5.79	-2.23	3.55
5	2.11	588	5.06	-5.76	-2.26	3.50

Table S1.4: Transition energies (ΔE_{01}, eV), wavelengths (λ_{01}, nm), oscillator strengths (f_{01}, dimensionless) relative to the $S_0 \rightarrow S_1$ transition, as well as frontier orbital energies and electronic gaps ($E_g = E_{LUMO} - E_{HOMO}$, all values in eV) calculated at the M06-2X/6-311G(d) level for increasingly large $(D\text{-}A)_n$ oligomers with A = DTBT.

n	ΔE_{01}	λ_{01}	f_{01}	E_{HOMO}	E_{LUMO}	E_g
			CPDT-DTBT			
1	2.76	449	0.96	-6.24	-1.96	4.28
2	2.49	498	2.54	-6.00	-2.08	3.92
3	2.41	516	4.20	-5.94	-2.12	3.82
4	2.38	521	5.90	-5.93	-2.13	3.79
5	2.35	527	7.46	-5.91	-2.15	3.77
			DTS-DTBT			
1	2.78	446	0.97	-6.30	-1.95	4.35
2	2.53	489	2.50	-6.08	-2.07	4.01
3	2.45	505	4.13	-6.02	-2.11	3.91
4	2.43	511	5.74	-6.01	-2.12	3.88
5	2.41	515	7.37	-5.99	-2.13	3.86
			DTP-DTBT			
1	2.76	449	0.92	-6.19	-1.94	4.25
2	2.49	497	2.43	-5.95	-2.05	3.90
3	2.41	514	4.06	-5.90	-2.10	3.80
4	2.38	520	5.67	-5.88	-2.11	3.77
5	2.37	523	7.23	-5.88	-2.12	3.76

Table S1.5: Transition energies (ΔE_{01}, eV), wavelengths (λ_{01}, nm), oscillator strengths (f_{01}, dimensionless) relative to the $S_0 \rightarrow S_1$ transition, as well as frontier orbital energies and electronic gaps ($E_g = E_{LUMO} - E_{HOMO}$, all values in eV) calculated at the M06-2X/6-311G(d) level for increasingly large $(D\text{-}A)_n$ oligomers with A = DPP.

n	ΔE_{01}	λ_{01}	f_{01}	E_{HOMO}	E_{LUMO}	E_g
			CPDT-DPP			
1	2.46	503	1.18	-6.08	-2.07	4.01
2	2.19	566	3.22	-5.94	-2.30	3.64
3	2.08	596	5.22	-5.90	-2.40	3.50
4	2.05	604	7.11	-5.89	-2.42	3.47
5	2.04	608	9.03	-5.89	-2.44	3.45
			DTS-DPP			
1	2.47	503	1.18	-6.10	-2.08	4.01
2	2.21	561	2.95	-5.97	-2.29	3.67
3	2.12	585	4.74	-5.93	-2.38	3.56
4	2.09	592	6.32	-5.93	-2.40	3.53
5	2.07	600	8.32	-5.91	-2.42	3.49
			DTP-DPP			
1	2.47	503	1.18	-6.05	-2.05	4.00
2	2.19	567	3.32	-5.89	-2.28	3.62
3	2.11	589	5.34	-5.87	-2.35	3.52
4	2.07	600	7.37	-5.86	-2.38	3.47
5	2.05	604	9.44	-5.86	-2.40	3.46

Table S1.6: Transition energies (ΔE_{01}, eV), wavelengths (λ_{01}, nm), oscillator strengths (f_{01}, dimensionless) relative to the $S_0 \rightarrow S_1$ transition, as well as frontier orbital energies and electronic gaps ($E_g = E_{LUMO} - E_{HOMO}$, all values in eV) calculated at the M06-2X/6-311G(d) level for increasingly large $(D\text{-}A)_n$ oligomers with A = DAP.

n	ΔE_{01}	λ_{01}	f_{01}	E_{HOMO}	E_{LUMO}	E_g
			CPDT-DAP			
1	2.18	568	1.12	-6.16	-2.62	3.54
2	1.91	649	3.19	-5.96	-2.76	3.19
3	1.81	685	5.22	-5.90	-2.83	3.07
4	1.76	704	7.20	-5.88	-2.86	3.02
5	1.74	714	9.24	-5.86	-2.87	2.99
			DTS-DAP			
1	2.19	565	1.10	-6.20	-2.62	3.58
2	1.92	647	3.00	-5.97	-2.76	3.21
3	1.85	670	4.71	-5.95	-2.81	3.14
4	1.81	683	6.46	-5.94	-2.83	3.10
5	1.80	689	8.38	-5.93	-2.84	3.09
			DTP-DAP			
1	2.17	570	1.13	-6.12	-2.60	3.51
2	1.91	650	3.23	-5.91	-2.75	3.17
3	1.80	688	5.29	-5.86	-2.81	3.05
4	1.76	705	7.30	-5.84	-2.84	3.00
5	1.73	715	9.34	-5.83	-2.85	2.97

Table S1.7: Transition energies (ΔE_{01}, eV), wavelengths (λ_{01}, nm), oscillator strengths (f_{01}, dimensionless) relative to the $S_0 \rightarrow S_1$ transition, as well as frontier orbital energies and electronic gaps ($E_g = E_{LUMO} - E_{HOMO}$, all values in eV) calculated at the M06-2X/6-311G(d) level for increasingly large $(D\text{-}A)_n$ oligomers with A = TII.

n	ΔE_{01}	λ_{01}	f_{01}	E_{HOMO}	E_{LUMO}	E_g
			CPDT-TII			
1	2.36	525	0.70	-6.03	-2.03	4.00
2	2.04	608	2.22	-5.77	-2.26	3.51
3	1.92	646	3.88	-5.70	-2.36	3.34
4	1.88	659	5.41	-5.68	-2.39	3.29
5	1.85	669	6.96	-5.66	-2.41	3.25
			DTS-TII			
1	2.38	520	0.68	-6.08	-2.03	4.05
2	2.07	598	2.17	-5.82	-2.25	3.57
3	1.96	631	3.80	-5.75	-2.34	3.41
4	1.90	651	5.33	-5.72	-2.39	3.33
5	1.91	649	6.78	-5.73	-2.39	3.34
			DTP-TII			
1	2.37	523	0.68	-6.01	-2.01	4.00
2	2.06	602	2.15	-5.74	-2.22	3.52
3	1.92	646	3.83	-5.64	-2.32	3.32
4	1.89	656	5.35	-5.63	-2.35	3.29
5	1.86	668	6.90	-5.62	-2.37	3.25

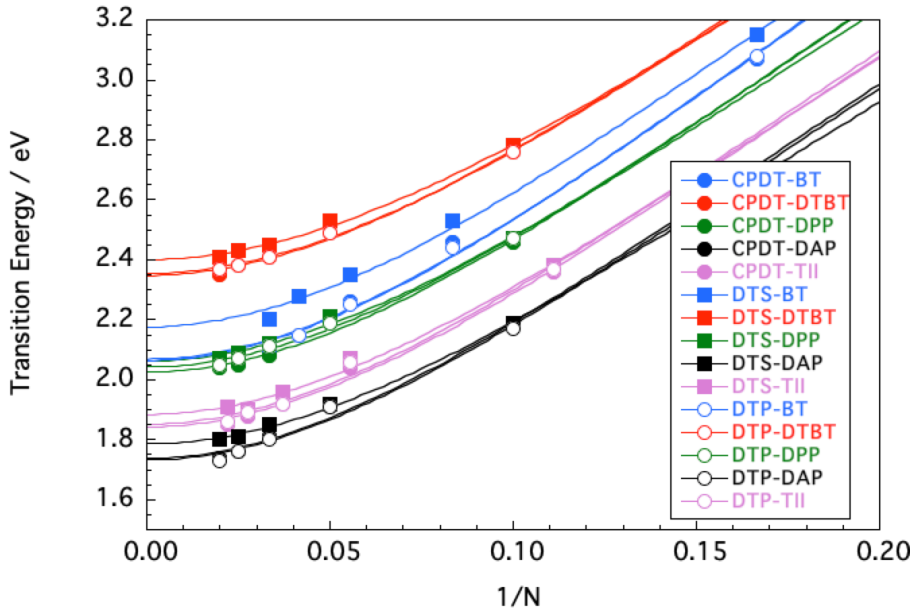

Figure S1.3: Evolution of vertical transition energies (eV) with chain length, as calculated at the M06-2X/6-311G(d) level. Lines are fits calculated according to the Kuhn's equation. The same marker stands for the same donor (D), the same color stands for the same acceptor (A). Optimized values of fitting parameters are given in Table S1.8. N is the number of conjugated double bonds in the polymer backbone.

Table S1.8: Transition energies in the polymer limit (ΔE_{01}^{∞}, eV) and optimized values of the Kuhn fit parameters D_k and E_0 (eV), as calculated at the M06-2X/6-311G(d) level for the investigated series of polymers.

Polymer	ΔE_{01}^{∞}	D_k	E_0
P(CPDT-BT)	2.07	-0.925	7.570
P(CPDT-DTBT)	2.30	-0.905	7.636
P(CPDT-DPP)	2.03	-0.923	7.297
P(CPDT-DAP)	1.74	-0.936	6.856
P(CPDT-TII)	1.85	-0.930	6.988
P(DTS-BT)	2.18	-0.918	7.600
P(DTS-DTBT)	2.40	-0.894	7.408
P(DTS-DPP)	2.07	-0.916	7.119
P(DTS-DAP)	1.79	-0.926	6.578
P(DTS-TII)	1.89	-0.925	6.989
P(DTP-BT)	2.07	-0.926	7.596
P(DTP-DTBT)	2.30	-0.903	7.570
P(DTP-DPP)	2.04	-0.921	7.248
P(DTP-DAP)	1.74	-0.935	6.817
P(DTP-TII)	1.88	-0.931	7.024

1.3 Light harvesting properties

As shown in Tables S1.3-S1.7, increasing n also induces successive hyperchromic shifts of the absorption band, as a result of the gradual increase of the oscillator strengths with the conjugation length. Since the oscillator strength is an extensive property that increases with oligomer length, we use the intensive property f_{01}/n, i.e. the oscillator strength divided by the number of repeating units, to provide more relevant comparisons between the different materials.

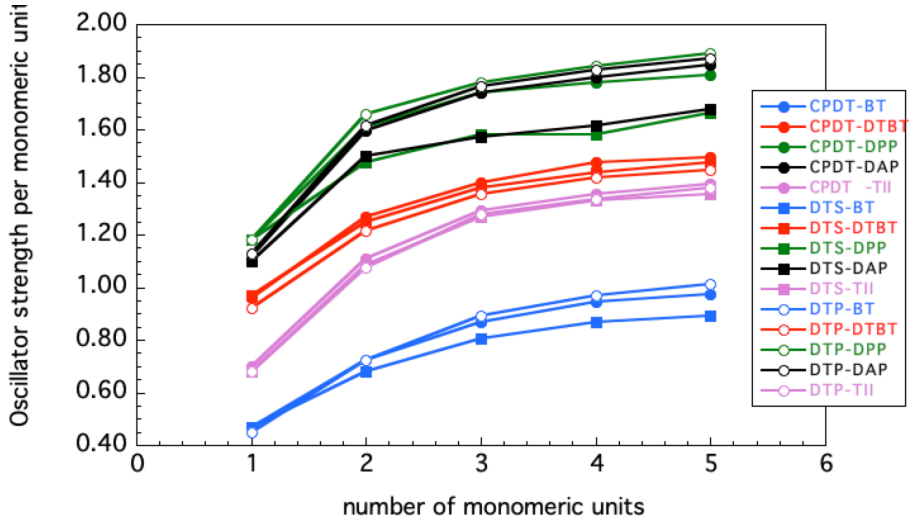

Figure S1.4: Evolution with chain length of oscillator strengths per monomer, calculated at M06-2X/6-311G(d) level. The same marker stands for the same donor (D), the same color stands for the same acceptor (A).

1.4 Solvent effects

Table S1.9: Transition energies (ΔE_{01}, eV), wavelengths (λ_{01}, nm), oscillator strengths (f_{01}, dimensionless) relative to the $S_0 \rightarrow S_1$ transition, as well as frontier orbital energies and electronic gaps ($E_g = E_{LUMO} - E_{HOMO}$, all values in eV) calculated at the IEFPCM:M06-2X/6-311G(d) level in chloroform for increasingly large $(D\text{-}A)_n$ oligomers with D = DTS.

n	ΔE_{01}	λ_{01}	f_{01}	E_{HOMO}	E_{LUMO}	E_g
			DTS-BT			
1	3.05	407	0.67	-6.67	-1.82	4.85
2	2.44	508	1.63	-6.28	-2.15	4.13
3	2.29	541	2.68	-6.15	-2.26	3.88
4	2.24	554	3.72	-6.10	-2.31	3.79
5	2.18	570	4.64	-6.05	-2.36	3.69
			DTS-DTBT			
1	2.69	461	1.22	-6.40	-2.03	4.37
2	2.48	499	2.66	-6.17	-2.13	4.04
3	2.43	511	4.24	-6.12	-2.17	3.95
4	2.41	514	5.81	-6.10	-2.18	3.92
5	2.40	516	7.40	-6.08	-2.19	3.90
			DTS-DPP			
1	2.28	544	1.40	-6.23	-2.21	4.02
2	2.08	595	2.93	-6.07	-2.39	3.68
3	2.03	612	4.56	-6.01	-2.45	3.56
4	2.02	614	6.03	-6.00	-2.46	3.54
5	2.00	620	7.98	-5.98	-2.48	3.50
			DTS-DAP			
1	1.96	634	1.38	-6.34	-2.80	3.53
2	1.74	714	2.96	-6.10	-2.93	3.17
3	1.71	724	4.53	-6.07	-2.97	3.10
4	1.69	732	6.08	-6.05	-2.98	3.06
5	1.69	734	7.85	-6.04	-2.99	3.05
			DTS-TII			
1	2.20	565	0.87	-6.22	-2.20	4.02
2	1.92	645	2.20	-5.96	-2.41	3.54
3	1.85	671	3.76	-5.88	-2.49	3.39
4	1.81	686	5.13	-5.84	-2.53	3.31
5	1.82	679	6.48	-5.85	-2.52	3.32

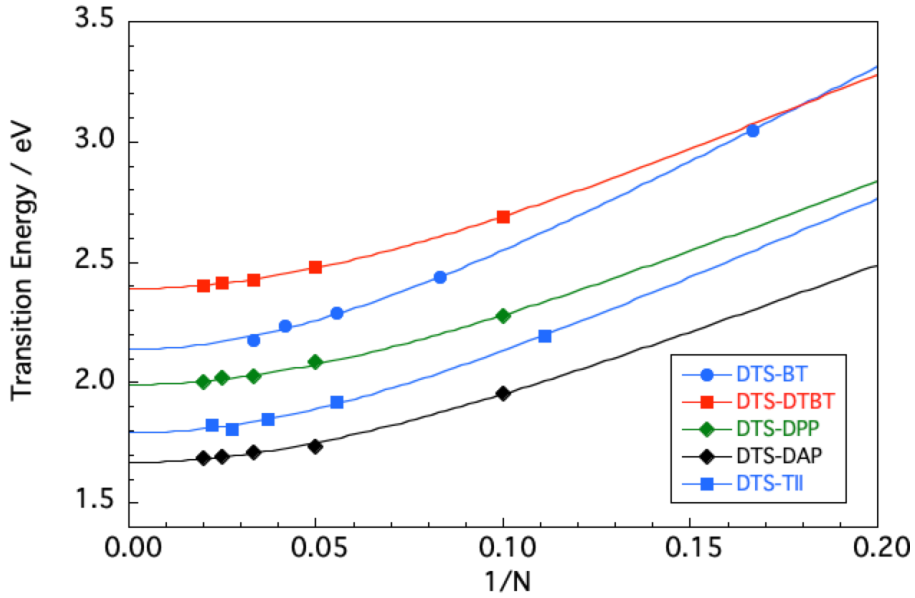

Figure S1.5: Evolution of vertical transition energies (eV) with chain length, as calculated at the IEFPCM:M06-2X/6-311G(d) level in chloroform for DTS-based derivatives. Lines are fits calculated according to the Kuhn's equation. N is the number of conjugated double bonds in the polymer backbone.

2. Synthesis and NMR data

N-dodecylthiophen-3-amine (linear)

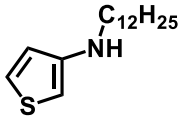

Synthesis: 3-bromothiophene (5 g, 2.87 mL, 30.7 mmol), dodecyldecan-1-amine (8,52 g, 34 mmol), copper (0,097 g, 1,533 mmol), copper(I) iodide (0,292 g, 1,533 mmol) and potassium phosphate tribasic (13,02 g, 61,3 mmol) were stirred in dimethyl aminoethanol (50 mL) at 80 °C for 48 h. The mixture was allowed to cool to room temperature, water (100 mL) was added and the solvent mixture was extracted with hexane. The hexane layer was dried over $MgSO_4$ and columned directly on silica gel using hexane as eluent. The solvent was removed under vacuum to give n-hexadecylthiophen-3-amine (linear) as a brown solid. (Yield = 35%)

NMR data: ^{1}H NMR (400 MHz, $CDCl_3$) δ (ppm) = 7.15 (dd, J_1= 4.92, J_2= 2.94, 1H), 6.62 (dd, J_1= 4.17, J_2= 3.25, 1H), 5.95 (dd, J_1= 5.27, J_2= 3.14, 1H), 3.58 (brs, 1H), 3.06 (t, J= 7.31 Hz, 2H), 1.61 (m, 4H), 1.45-1.06 (m, 16H), 0.88 (t, J= 6.51 Hz, 3H).

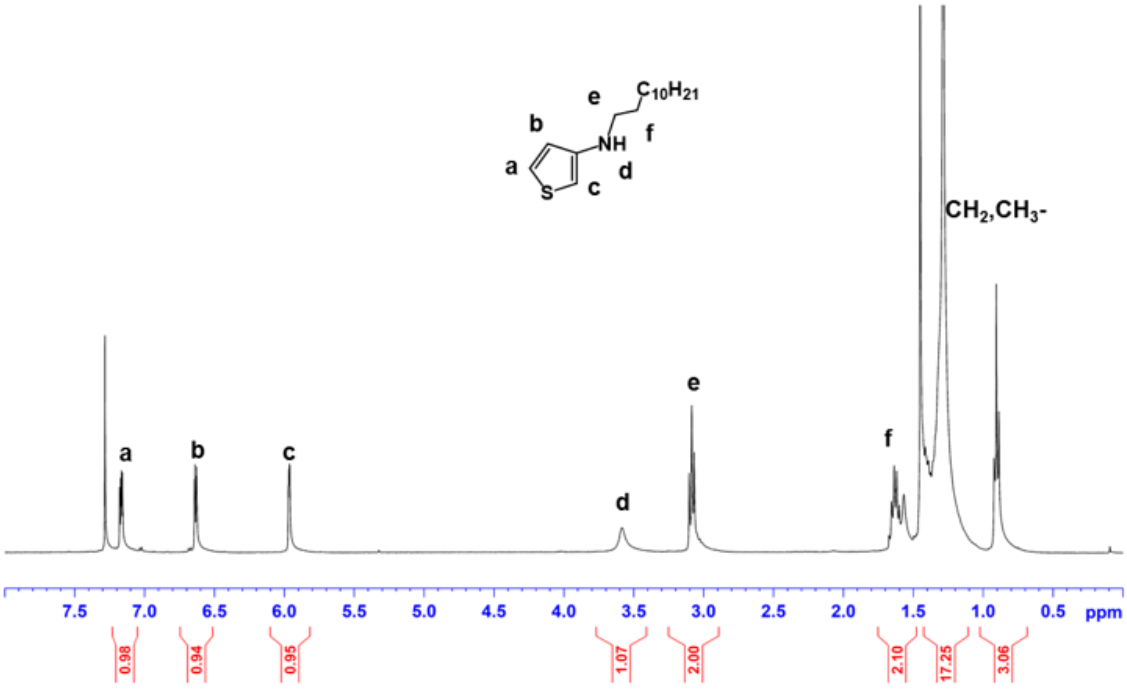

Figure S2.1: ^{1}H NMR spectrum of N-Dodecylthiophen-3-amine (400 MHz, $CDCl_3$).

4-(dodecyl)-4H-thieno[3,2]pyrrole-5,6-dione (linear)

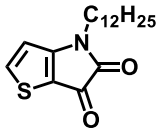

Synthesis: N-dodecylthiophen-3-amine (2,92 g, 10,94 mmol) in anhydrous DCM (30 mL) was added dropwise to oxalyl chloride (1,29 mL, 10,64 mmol) in anhydrous DCM (20 mL) at 0°C. After 30 minutes, triethylamine (7,91 mL, 56,8 mmol) in anhydrous DCM (5 mL) was added dropwise and stirred overnight at room temperature. The solvent was removed under vacuum and crude product was purified by chromatography on silica gel in DCM. 4-(dodecyl)-4H-thieno[3,2]pyrrole-5,6-dione (linear) was obtained as red solid.

NMR data: ^{1}H NMR (400 MHz, $CDCl_3$) δ (ppm) = 8.00 (d, J = 4.9 Hz, 1H), 6.78 (d, J = 5.0 Hz, 1H), 3.65 (t, J = 7.2 Hz, 2H), 1.67 (p, J = 6.9 Hz, 2H), 1.38- 1.22 (m, 18H), 0.87 (t, J = 6.6 Hz, 3H)

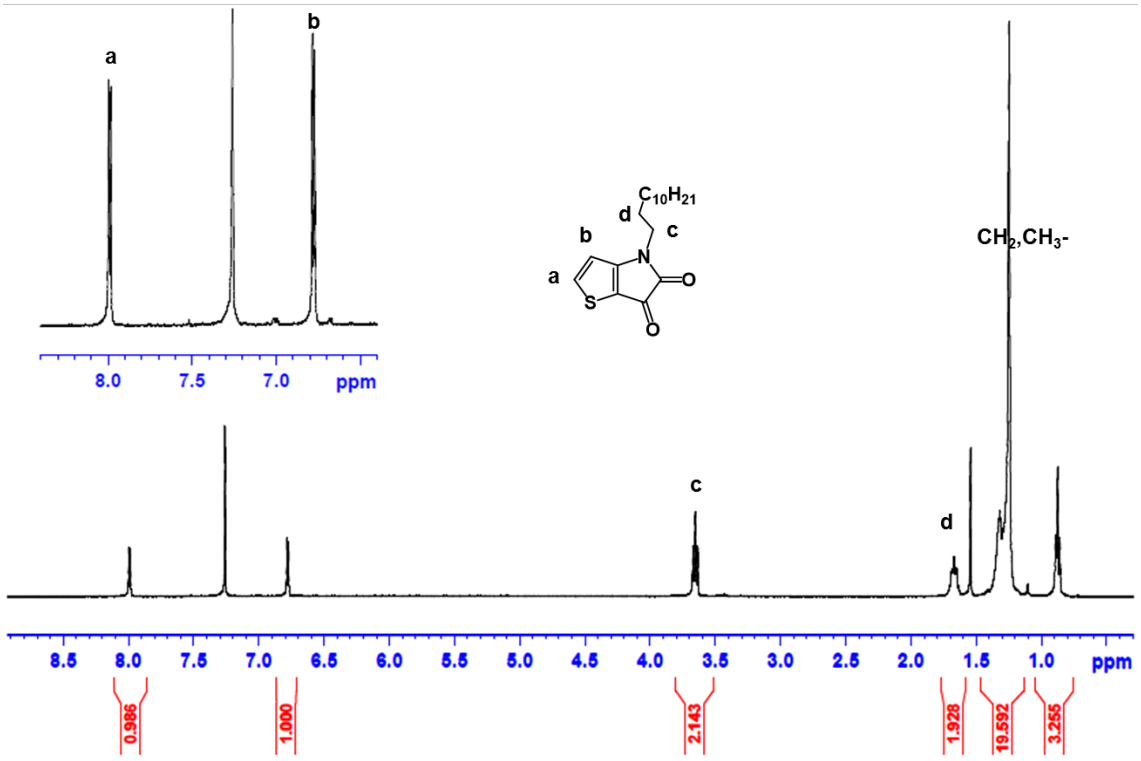

Figure S2.2: ^{1}H NMR spectrum of 4-(Dodecyl)-4H-thieno[3,2-b]pyrrole-5,6-dione (400 MHz, $CDCl_3$).

(E)-4,4'-didodecyl-[6,6'-bithieno[3,2- b]pyrrolylidene]-5,5'(4H,4'H)-dione (linear)

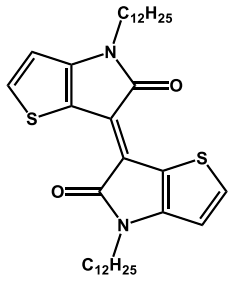

Synthesis: A solution of 4-(dodecyl)-4H-thieno[3,2-b]pyrrole-5,6-dione (0,35 g, 1,87 mmol) and Lawesson's Reagent (0,379 g, 0,936 mmol) in toluene (15 mL) was stirred at 65°C for 6 h. Progress change of reaction was monitored by TLC and change in color (from red to violet blue). The reaction mixture was then cooled down to room temperature. After removing the solvent under vacuum, the crude product was purified by flash chromatography on silica gel using hexane: DCM as eluent. The solvent was removed under vacuum to give the product as a purple solid. (Yield = 70%)

NMR data: ^{1}H NMR (400 MHz, $CDCl_3$) δ (ppm) = 7.53 (d, J = 5.3 Hz, 2H), 6.81 (d, J = 5.1 Hz, 2H), 3.80 (t, J = 7.3 Hz, 4H), 1.73 (m, 4H), 1.40-1.16 (m, 36H), 0.87 (t, J = 6.61 Hz, 6H).

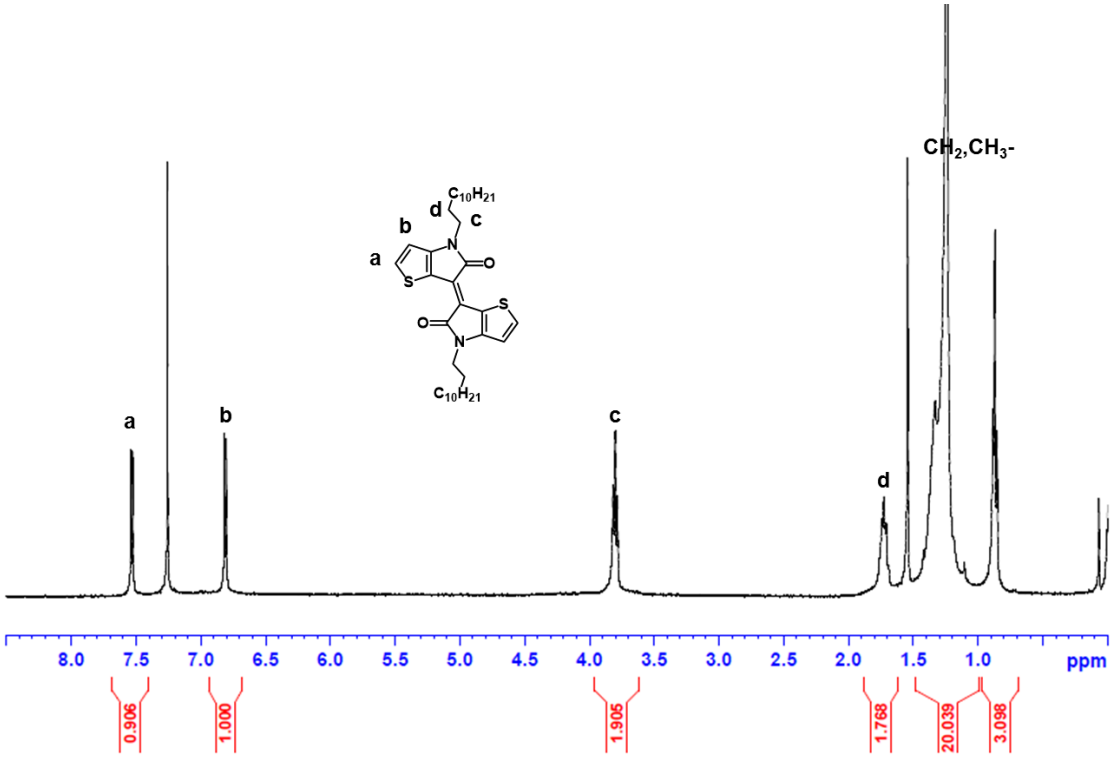

Figure S2.3: ^{1}H NMR spectrum of (E)-4,4'-didodecyl-[6,6'-bithieno[3,2- b]pyrrolylidene]-5,5'(4H,4'H)-dione (400 MHz, $CDCl_3$).

(E)-2,2'-dibromo-4,4'-didodecyl[6,6'bithieno[3,2b]pyrrolidene]5,5'(4H,4H')-dione (linear)

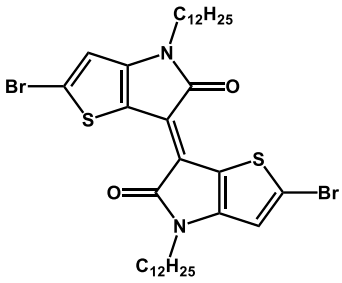

To an ice cold solution of (E)-4,4'-dihexadecyl-[6,6'-bithieno[3,2-b]pyrrolylidene]-5,5'(4H,4'H)-dione (0,415 g, 0,57 mmol) in DCM (25 mL), NBS (0,22 g, 1,26 mmol) in THF (1 mL) was added dropwise over 30 minutes. The reaction progress was monitored by TLC. After completion, reaction was quenched by the addition of water (10 mL) and dichloromethane (50 mL) and the organic layer was separated off. The organic layer was washed with water (2 x 10 mL), brine (10 mL) and dried over $MgSO_4$. After filtering off the $MgSO_4$ and removing the solvent under vacuum, the crude product was purified by chromatography on silica gel using hexane and DCM as eluent. After removal of solvent, the crude product was purified by chromatography on silica gel using a hexane: DCM mixture as eluent. The solvent was removed under vacuum to give the product as a blue solid which was further purified by washing with methanol and dried under high vacuum to give the product. (Yield = 80%)

NMR data: ^{1}H NMR (400 MHz, $CDCl_3$) δ (ppm) = 6.86 (s, 2H), 3.74 (t, J =7.3 Hz, 4H), 1.69 (m, 4H), 1.38-1.19 (m, 36H), 0.87 (t, J = 6.54 Hz, 6H). ^{13}C NMR (75 MHz, $CDCl_3$): δ 170.09, 149.87, 123.23, 119.76, 114.66, 41.87, 31.92, 29.61, 29.48, 29.344, 29.22, 28.566, 26.85, 22.69, 14.13

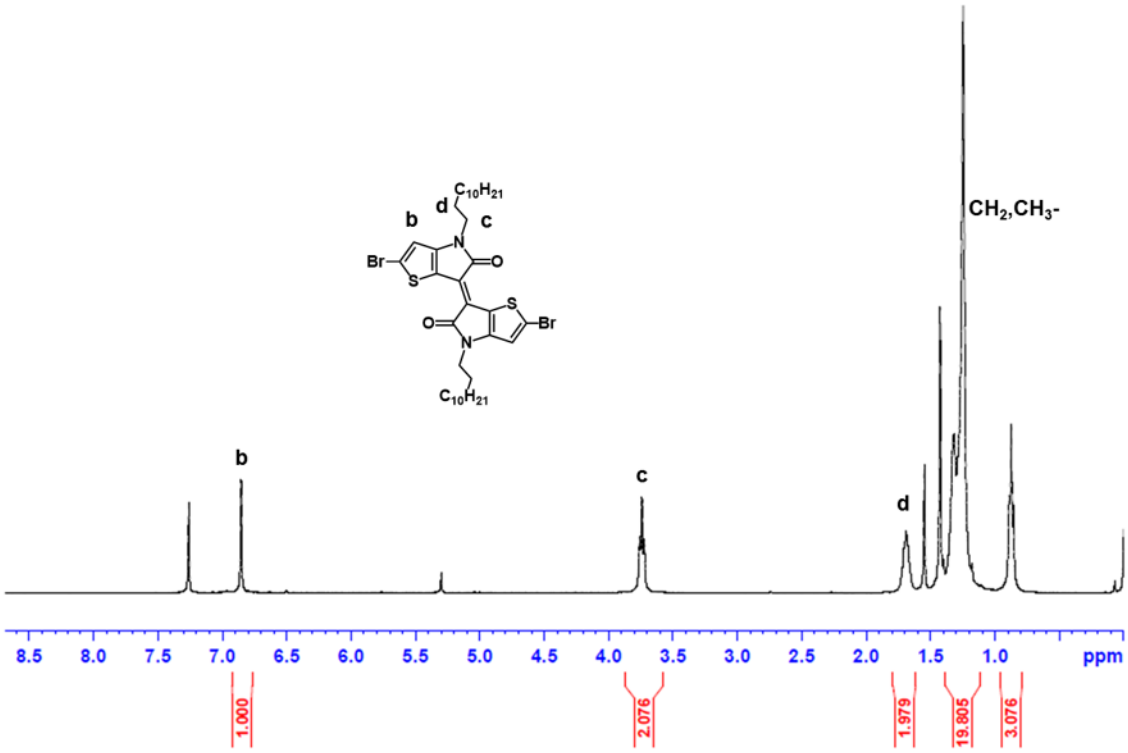

Figure S2.4: ^{1}H NMR spectrum of (E)-2,2'-dibromo-4,4'-didodecyl-[6,6'- bithieno[3,2 b]pyrrolylidene]-5,5'(4H,4'H)-dione [5] (400 MHz, $CDCl_3$).

P(DTS-TII)

NMR data: ^{1}H NMR (400 MHz, $CDCl_3$) δ (ppm) = 7.7-6.7 (H aromatic, a et b, 4H/repetitive units), 3.8 (CH_2-N, c, 4H/repetitive units), 2.1-0.5 (H aliphatic, d, 80H/repetitive units).

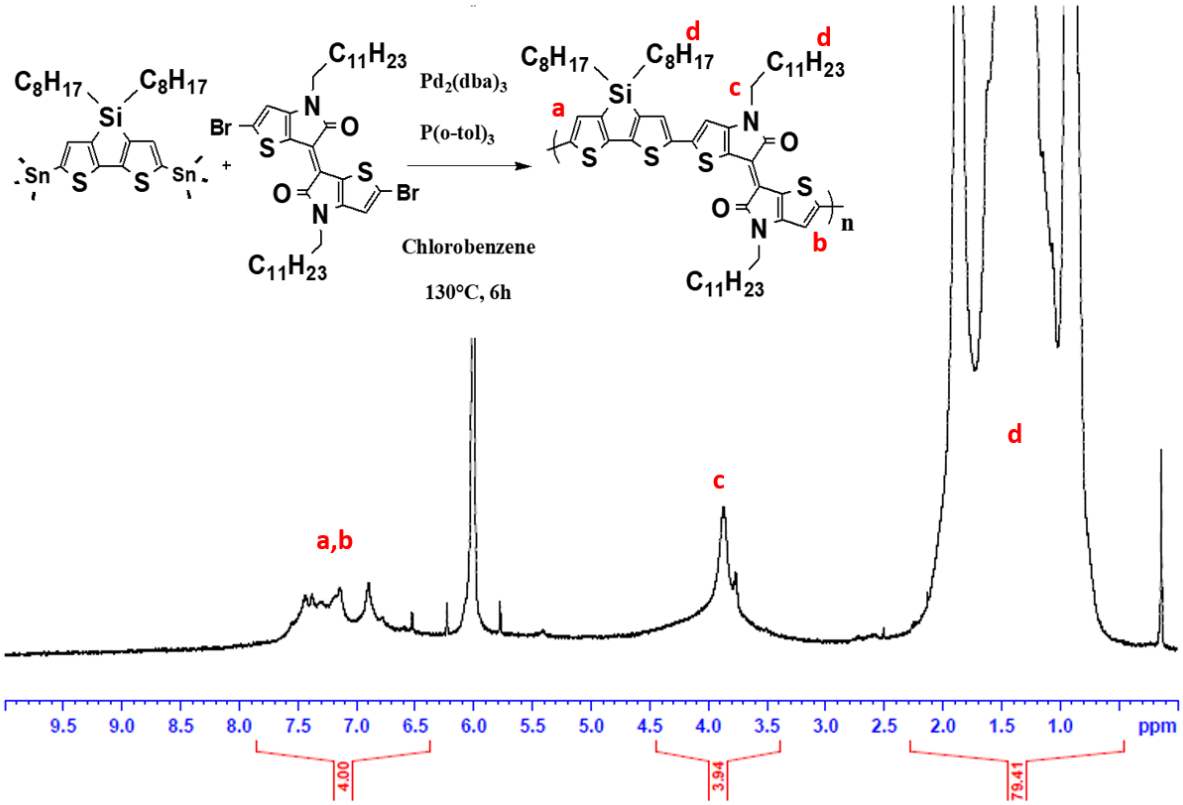

Figure S2.5: ^{1}H NMR spectrum of P(DTS-TII) (400 MHz, $CDCl_3$).

Diketopyrrolopyrrole (DPP) monomer

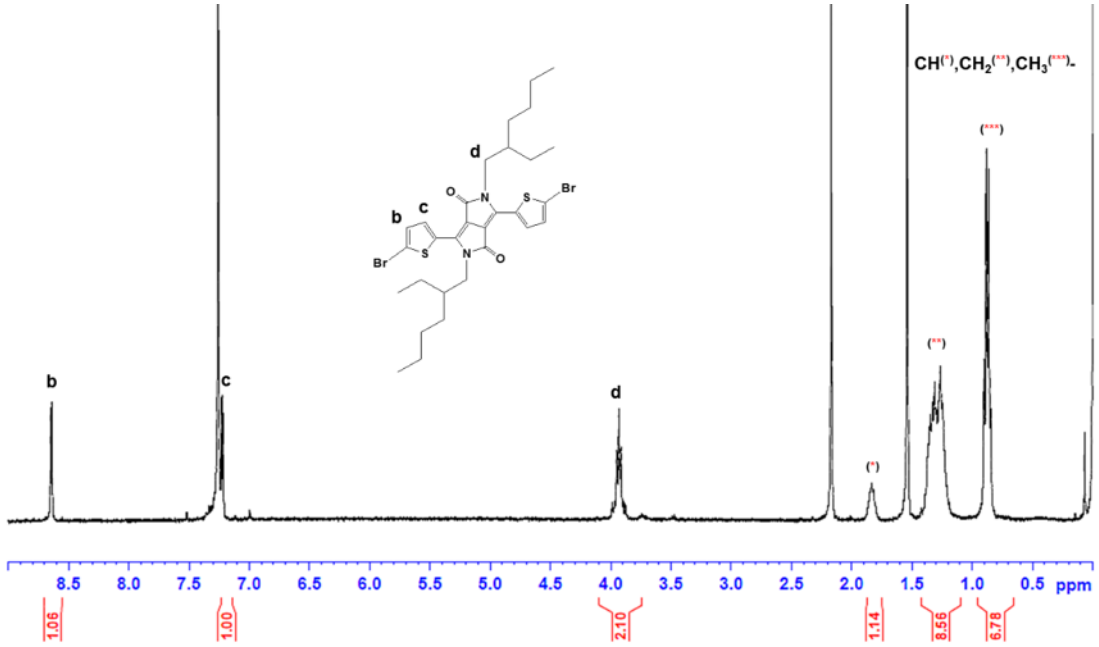

Figure S2.6: ^{1}H NMR spectrum of the DPP monomer.

2,5-diazapentalene (DAP) monomer

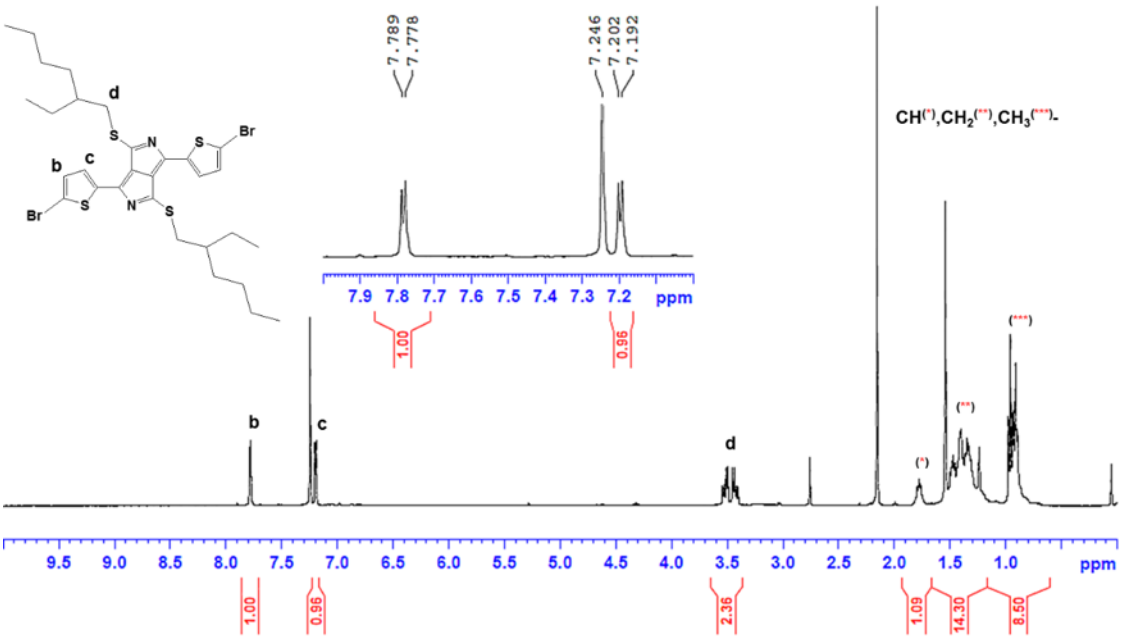

Figure S2.7: ^{1}H NMR spectrum of the DAP monomer.

Benzothiadiazole (BT) monomer

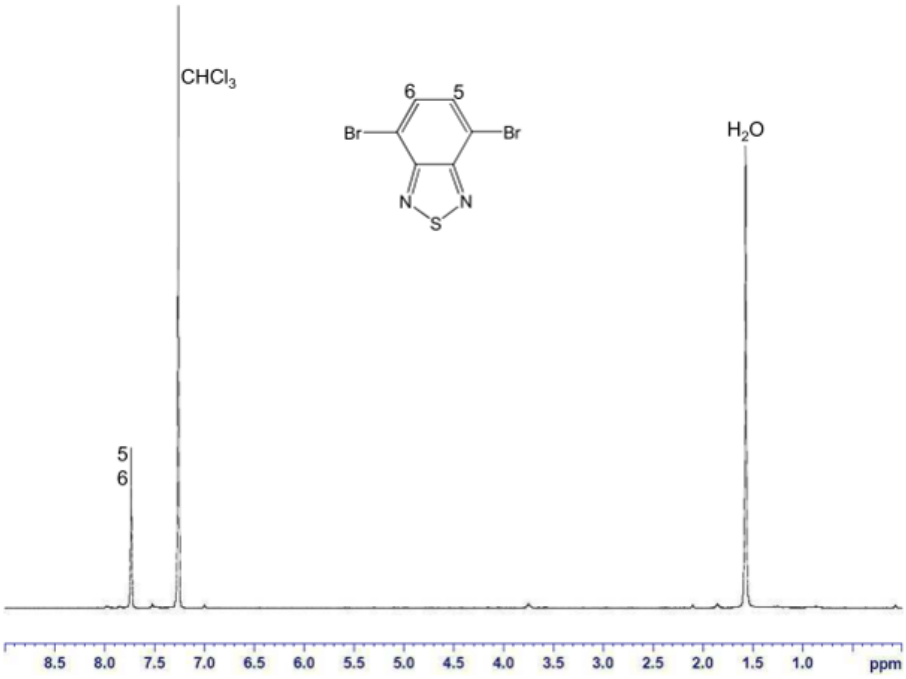

Figure S2.8: ^{1}H NMR spectrum of BT (400 MHz, $CDCl_3$).

Di(thiophen-2-yl)-2,1,3-benzothiadiazole (DTBT) monomer

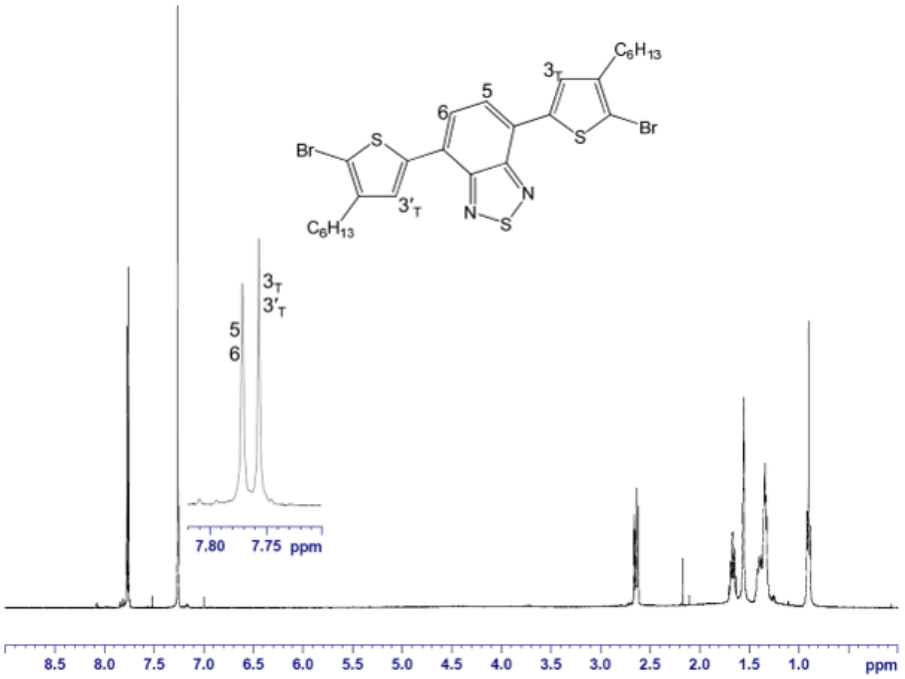

Figure S2.9: ^{1}H NMR spectrum of DTBT (400 MHz, $CDCl_3$).

P(DTS-DPP)

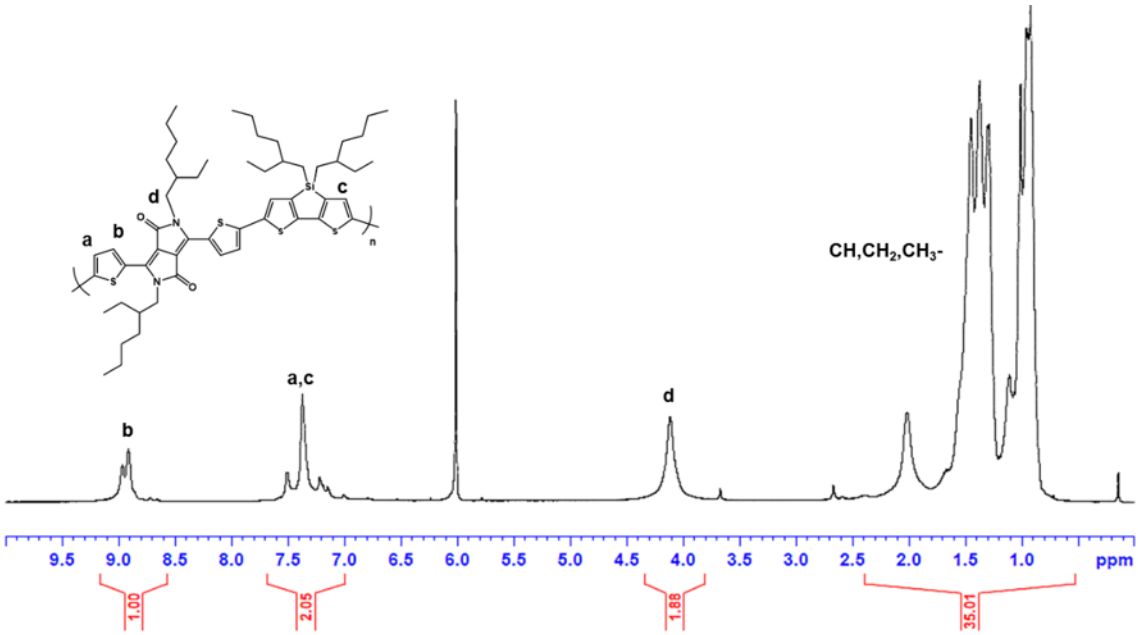

Figure S2.10: ^{1}H NMR spectrum of P(DTS-DPP).

P(DTS-DAP)

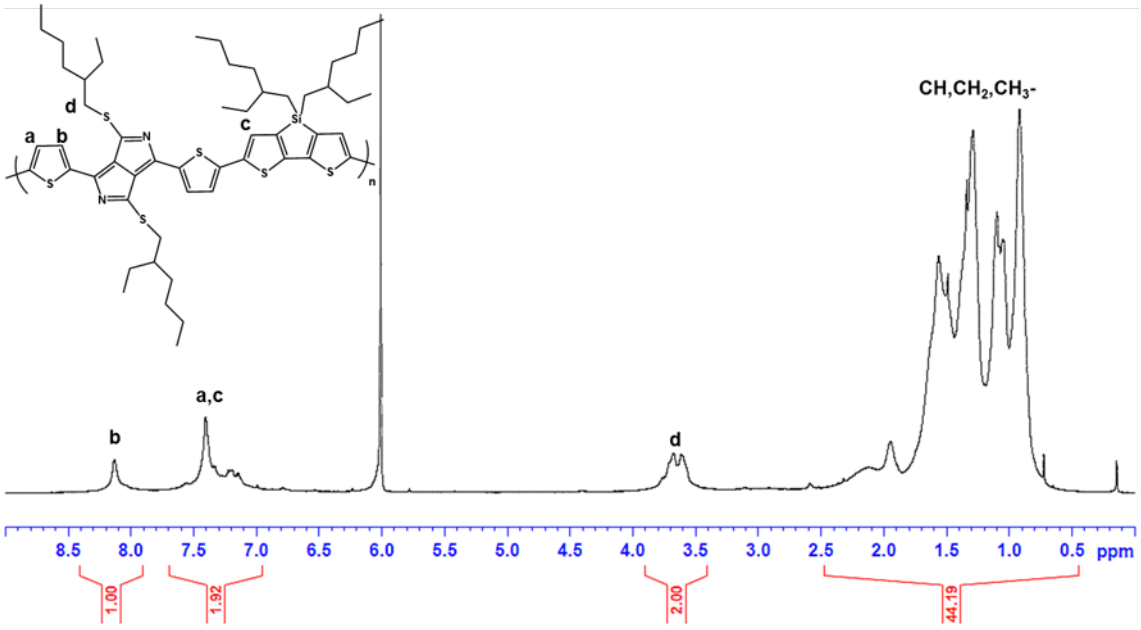

Figure S2.11: ^{1}H NMR spectrum of P(DTS-DAP).

3. Cyclic Voltammetry

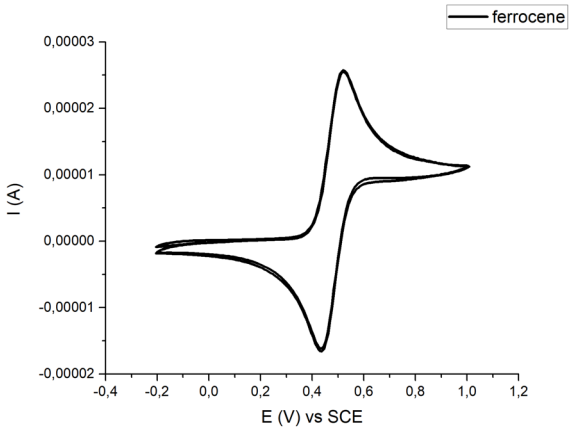

Figure S3.1: CV of Ferrocene performed in 0.1 M Bu_4NPF_6/CH_3CN using a sweep rate of 0.1 $V.s^{-1}$.